JOURNAL OF MATERIALS SCIENCE 6 (1971) 361-376

The Orientation Dependence of the Deformation Modes of Crystalline Mercury at 77°K

J. S. ABELL*, A. G. CROCKER, D. M. M. GUYONCOURT†
Department of Physics, University of Surrey, Guildford, UK

Single crystals of mercury have been deformed either uniaxially or in four-point bending at 77°K and the orientation dependence of the operative deformation modes investigated. The experimental techniques adopted are briefly described and results presented for thirty-five specimens. The predominant deformation mode was crystallographic $\{11\bar{1}\}\langle 1\bar{1}0$* slip but '$\{\bar{1}35\}$' twinning and $\{1\bar{1}0\}$ kinking were frequently observed. Slip in the close-packed $\langle 011\rangle$ direction was wavy and restricted to three specimens. The orientation dependence of these deformation modes is interpreted using Schmid-factor contour-plots of the first- and second-most highly stressed variants. The form and nature of the boundaries between different regions of these plots are discussed in detail. The operative deformation modes in the bent specimens can be satisfactorily interpreted by making use of a new analysis of plane plastic strain developed as a result of this work. The results on deformation kinking have also led to a new general theory of the crystallography of this phenomenon. A critical resolved shear stress of 18 ± 2 g mm^{-2} was found for $\{11\bar{1}\}\langle 1\bar{1}0\rangle$ slip for specimens with Schmid-factors greater than about 0.3. Much larger values were measured or deduced for other specimens and possible explanations of this surprising result are advanced. Several of the observations are considered to be of general importance to the understanding of the mechanical properties of all crystalline materials but they can only be thoroughly investigated on a material, like mercury, of comparatively low crystal symmetry.

1. Introduction

Recently the deformation modes of crystalline mercury have been the subject of a series of investigations at the University of Surrey [1]. Experiments have been performed over a range of temperatures from near the melting point of 234°K to liquid-helium temperature on slip, twinning, kinking and a stress-induced phase transformation. It has been established that, referring the crystal structure of mercury to the convenient face-centred rhombohedral cell of axial angle 98° 22′ [2], the predominant slip direction at all temperatures is $\langle 1\bar{1}0\rangle$, the corresponding slip plane being $\{11\bar{1}\}$ [3-6] except near the melting point where non-crystallographic slip can occur [7]. Wavy slip in the most closely packed $\langle 011\rangle$ direction is also common at these higher temperatures [4, 7]. Deformation-twinning occurs at temperatures below about 170°K on an irrational plane near $\{\bar{1}35\}$, the shear direction being $\langle\bar{1}21\rangle$ and the shear strain 0.633 [8-10]. In addition, crystals deformed at 20°K and below [5, 6, 11] exhibit a stress-induced phase transformation, the habit plane and shear direction of the product plates being approximately $\{\bar{1}13\}$ and $\langle 110\rangle$ respectively. Finally, in the series of experiments to be described in the present paper, detailed information has been obtained for the first time on kinking, both as an accommodation effect and as a macroscopic deformation mode. These kinks have their boundaries parallel to the $\{1\bar{1}0\}$

*Now at Department of Physical Metallurgy, University of Birmingham.
†Now at British Non-Ferrous Metals Research Association, Euston Road, London, NW1.

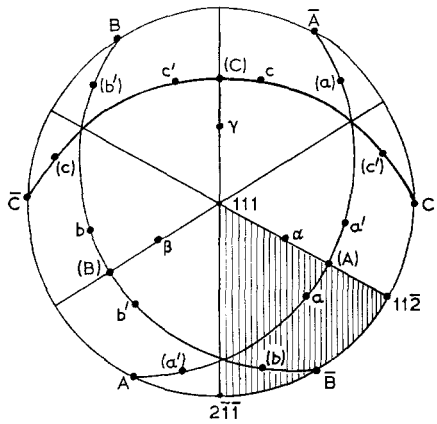

Figure 1 Standard 111 stereogram for crystalline mercury illustrating the letter notation for the elements of the slip, twinning and kinking modes defined in table I. The standard unit triangle is shown shaded.

TABLE I

Shear element	Letter notation for variants		
$\langle 1\bar{1}0\rangle$	A = $[1\bar{1}0]$;	B = $[\bar{1}01]$;	c = $[01\bar{1}]$
$\langle 110\rangle$	α = [110];	β = [101];	γ = [011]
$\{11\bar{1}\}$	(A) = $(11\bar{1})$;	(B) = $(1\bar{1}1)$;	(C) = $(\bar{1}11)$
$\langle 21\bar{1}\rangle$	a = $[21\bar{1}]$;	b = $[1\bar{1}2]$;	c = $[\bar{1}21]$
	a′ = $[12\bar{1}]$;	b′ = $[2\bar{1}1]$;	c′ = $[\bar{1}12]$
$'\{\bar{3}5\bar{1}\}'$	(a) = $'(\bar{3}5\bar{1})'$;	(b) = $'(5\bar{1}\bar{3})'$;	(c) = $'(\bar{1}\bar{3}5)'$
	(a′) = $'(5\bar{3}\bar{1})'$;	(b′) = $'(\bar{3}\bar{1}5)'$;	(c′) = $'(\bar{1}5\bar{3})'$
$'\langle 33\bar{2}\rangle'$	(A) = $'[33\bar{2}]'$;	(B) = $'[3\bar{2}2]'$;	(C) = $'[\bar{2}33]'$
$\{1\bar{1}0\}$	A = $(1\bar{1}0)$;	B = $(\bar{1}01)$;	C = $(01\bar{1})$

The letter notation used for the shear elements of the operative slip, twinning and kinking modes. Approximations to rational elements are indicated by apostrophes.

mirror plane, which is perpendicular to the predominant $\langle 1\bar{1}0\rangle$ slip direction, and the effective shear direction is initially the normal to the operative $\{1\,1\,\bar{1}\}$ slip plane, which is irrational but approximately $\langle 3\,3\,\bar{2}\rangle$. Kinks with irrational shear directions have not been reported previously and the crystallography of this deformation mechanism will be the subject of a further paper [12].

Throughout the course of these experiments on crystalline mercury, information has been collected on the orientation dependence of the occurrence of the operative deformation modes. Indeed some early results on $\langle 1\bar{1}0\rangle$ and $\langle 0\,1\,1\rangle$ slip obtained from single-crystal specimens deformed in tension at either 210 or 90°K were published by Rider and Heckscher [4] and some corresponding results for the phase transformation have been given by Abell and Crocker [5]. However, the bulk of our results have not been published and in the present paper we summarise the data on the orientation dependence of slip, twinning and kinking obtained at 77°K from single crystals deformed in tension, compression or bending and discuss these in terms of the geometry of the deformation processes. To do this we first introduce in section 2 a convenient letter-notation for the shear elements of the operative deformation modes and use this in presenting contour-plots for the Schmid-factors of these modes for crystals oriented in the standard stereographic unit triangle. The deformation geometry of plane plastic bending is also discussed in this section. Then in section 3 we describe the experimental techniques adopted. This is followed in sections 4.1 and 4.2 by our experimental results for the uniaxial tension and compression tests and the more complex bending tests. These are discussed in section 4.3 and finally the implications of the results of the paper on general analyses of plastic deformation of all crystalline materials are examined in section 5.

2. Deformation Geometry for Single Crystals of Mercury

The face-centred rhombohedral unit cell of crystalline mercury has three $\{1\bar{1}0\}$ mirror planes in addition to the [1 1 1] three-fold axis. Thus the standard 1 1 1 stereogram may be divided into six unit triangles as illustrated in fig. 1. The locations of the poles of directions and planes on this stereogram are then defined by the cosine c of the rhombohedral angle which is -0.1454 or approximately $-\frac{1}{7}$. Note that apart from [1 1 1] and directions in (1 1 1), the poles of planes and directions with the same indices do not coincide. The six crystallographically equivalent variants which in general arise for each plane and direction can result in confusion when the Miller index notation is adopted. It has therefore been found convenient to introduce a letter convention which is illustrated in fig. 1 and defined fully in table I. In this notation the slip directions $\langle 1\bar{1}0\rangle$ and $\langle 0\,1\,1\rangle$ and the twinning directions $\langle\bar{1}\,1\,2\rangle$ are represented by upper case Roman, lower case Greek and lower case Roman letters respectively. Only three letters are required for the three variants of the slip directions and by using primed and unprimed letters this is also true for the twinning directions. Bracketed upper and lower case Roman letters

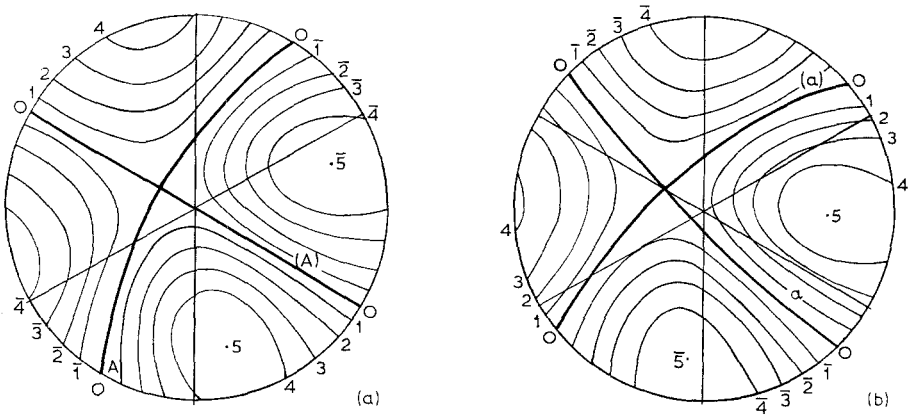

Figure 2 Complete stereographic plots of Schmid-factor contours, in units of 10^{-1}, for (a) the (A) A or $(11\bar{1})$ $[1\bar{1}0]$ slip system, which is equivalent to the A (A) or $(1\bar{1}0)'$ $[33\bar{2}]'$ kinking mode and (b) the (a) a twinning mode Negative factors are indicated by bars.

are used for the crystallographic $\{1\,1\,\bar{1}\}$ slip planes and the irrational $'\{\bar{1}\,\bar{3}\,5\}'$ twinning planes associated with the corresponding $\langle 1\,\bar{1}\,0\rangle$ and $\langle\bar{1}\,1\,2\rangle$ shear directions respectively. A particular $\langle 0\,1\,1\rangle$ shear direction does not lie in the corresponding $\{1\,1\,\bar{1}\}$ plane, but it is contained in the remaining two variants of this plane. Each pair of primed and unprimed twinning directions has a common conjugate twinning plane of the form $\{1\,1\,\bar{1}\}$ [9, 10] defined by the associated upper case letter. The effective shear direction and plane of a macroscopic kink are parallel to the shear plane and direction respectively of the corresponding $\{1\,1\,\bar{1}\}\langle 1\,\bar{1}\,0\rangle$ slip system and are therefore allocated the same letters. Finally, negative planes and directions are indicated by bars. Thus for example the $[1\,\bar{1}\,0]$, $[1\,1\,0]$, $[2\,1\,\bar{1}]$, $[1\,2\,\bar{1}]$, $'[3\,3\,\bar{2}]'$ and $[\bar{1}\,1\,0]$ directions are given by A, α, a, a′, (A) and $\bar{\text{A}}$ respectively and the planes $(1\,1\,\bar{1})$, $'(5\,\bar{3}\,1)'$ and $(1\,\bar{1}\,0)$ by (A), (a) and A. Also α lies in (B) and (C) and the conjugate twinning plane of a and a' is (A). Note from fig. 1 that A, (a′), a, a′, (a) and $\bar{\text{A}}$ lie on a single great circle which, when the approximation $c = -\frac{1}{7}$ is adopted, also contains (A).

Having defined the deformation modes which are known to operate in crystalline mercury, we shall now proceed to consider which variants of these modes are likely to occur in single crystals of particular orientations deformed in specified ways. The most convenient way of performing this task is to compare stereographic contour plots of the Schmid-factors of the possible shear systems. Thus in figs. 2a and b we give the appropriate plots for the (A) A or $(1\,1\,\bar{1})$ $[1\,\bar{1}\,0]$ slip system, which is equivalent to the A (A) or $(1\,\bar{1}\,0)$ $'[3\,3\,\bar{2}]'$ kinking mode, and for the (a) a or $'(\bar{3}\,5\,\bar{1})'$ $[2\,1\,\bar{1}]$ twinning mode. No corresponding plot for the α or $[1\,1\,0]$ direction has been given as the slip plane is not well defined [4, 7]. The signs of the Schmid-factors in fig. 2 are such that a positive value implies that in a tensile test the positive side of the shear plane is displaced in the positive shear direction. These signs are of course crucial for deformation twinning, which is a unidirectional shear process, so that positive Schmid-factors indicate that this particular variant of the twinning mode may occur in tension but not in compression and vice versa for negative values. The signs may also be significant for slip if an asymmetry of dislocation movement in opposite directions can exist. In mercury this asymmetry should not arise for (A) A type slip as the $\langle 1\,\bar{1}\,0\rangle$ slip direction is a two-fold axis but it can in principle occur for the α or $\langle 0\,1\,1\rangle$ type slip direction [7].

The contour-plots of fig. 2 are for particular variants of the deformation modes. In practice we will wish to know which variants of a mode are likely to occur. This may be conveniently illustrated by plotting the Schmid-factor contours for the highly stressed variants of a particular deformation mode in the unit triangle shown shaded in fig. 1. This has been done in fig. 3 for the first and second most highly stressed variants. Here plots a and b are for the (A) A or $\{1\,1\,\bar{1}\}\langle 1\,\bar{1}\,0\rangle$ type slip modes and are valid for both tension and compression tests. However for twinning, owing to the unidirectional shear direction, separate contour-plots are necessary

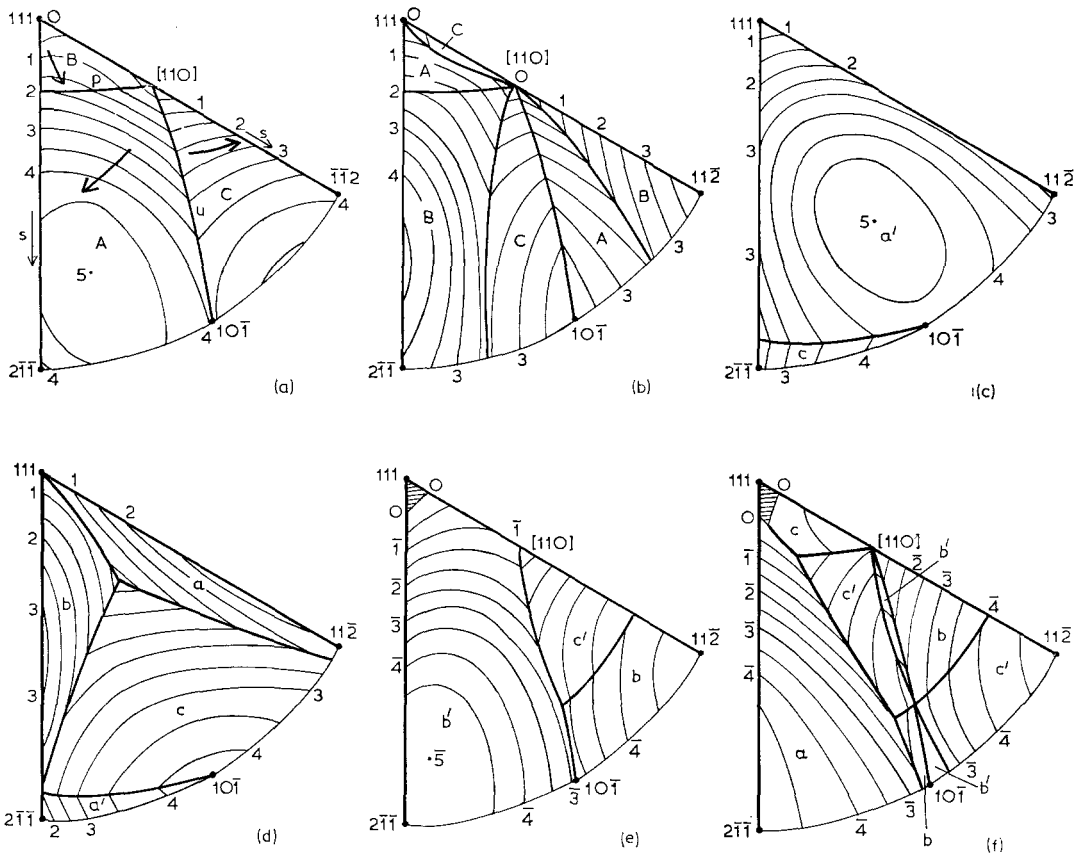

Figure 3 Schmid-factor contour-plots on the standard stereographic unit triangle, for the $\{11\bar{1}\}\langle 1\bar{1}0\rangle$ slip and '$\{\bar{1}\bar{3}5\}$' twinning modes of crystalline mercury. Units of 10^{-1} have been used and negative factors are represented by bars. Plots (a) and (b) are for slip in either compression or tension, (c) and (d) are for twinning in tension and (e) and (f) are for twinning in compression, the most highly stressed system preceding the second most highly stressed in each case. The boundaries between regions in which different variants of the deformation modes operate are indicated by bold lines and the regions are labelled with the code letter of the shear direction. In (a) the stable, unstable and permeable boundaries are labelled s, u and p respectively and the sense of rotation of the axes of specimens tested in tension is represented by bold arrows. There are no available deformation modes in the shaded regions of plots (e) and (f).

for tension and compression and these are given in plots c to f. In all of these cases the unit triangle is subdivided into separate regions in which different variants of the deformation mode being considered are favoured. The variants are distinguished by the code letters of their shear directions. Note that plots a and b show that all variants of $\{11\bar{1}\}\langle 1\bar{1}0\rangle$ type slip have a zero Schmid-factor for crystals oriented along either [111] or [110]. Similarly there is a region near [111] shown shaded in plot e for which twinning in compression should not occur. Indeed, a marked difference between twinning in tension and compression is clearly demonstrated by the pairs of plots. In particular one variant of the twinning mode occupies most of the unit triangle in plot c whereas in plot d this same region is divided into three major sectors.

The form of the boundaries between the regions in fig. 3 makes a fascinating study. These boundaries, which are represented by bold lines, are in general segments of curves representing cones of directions for which the Schmid-factors for two variants of a deformation mode are equal in magnitude. However, from elementary symmetry arguments the $\{1\bar{1}0\}$ mirror planes must be examples of these curves, indicating that in particular cases the cones degenerate into a

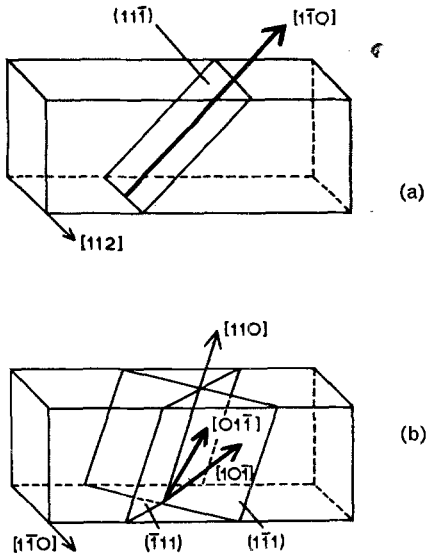

Figure 4 Single- and double-shear bending orientations for (A) A or $\{1\,1\,\bar{1}\}\langle 1\,\bar{1}\,0\rangle$ type slip of crystalline mercury. The bend axes [1 1 2] and [1 $\bar{1}$ 0] for the single- and double-shear cases are indicated in (a) and (b) respectively together with the operative slip planes and shear directions (shown bold).

pair of planes. Thus in fig. 3a the straight edges of the unit triangle, representing the traces of $\{1\,\bar{1}\,0\}$ planes, form boundaries of regions and the remaining curved boundaries are segments of the traces of the $\{1\,1\,\bar{1}\}$ planes. These boundaries which arise when the two Schmid-factors have the same sign are repeated in fig. 3b but with the associated shear systems transposed. However, additional boundaries are introduced, this time all being segments of the projection of a true cone, which arises when the associated Schmid-factors have opposite signs. Similar characteristics arise in figs. 3c-f, except that as these contour-plots are related to a twinning rather than a slip mode, Schmid-factors of opposite sign are not allowed. The boundaries for the primary systems are again repeated in the plots for the secondary systems together with additional boundaries. The traces of the $\{1\,\bar{1}\,0\}$ planes form boundaries, as do three other great circles representing planes which contain specimen axes. In particular the $\{1\,1\,\bar{1}\}$ plane again occurs; it arises from complementary pairs of twins for which $\{1\,1\,\bar{1}\}$ is the conjugate twinning plane and is represented by the b-b′ and c-c′ boundaries in fig. 3f. The other two planes are irrational, the first being represented by the c-a′ and b-c′ boundaries in figs. 3d and f respectively and the second by the a-c′ boundary in fig. 3f. The remaining boundaries are segments of the cone associated with pairs of variants related by the three-fold axis. Note that the curved edges of the unit triangles in fig. 3 do not divide regions in which different shear systems operate and are not therefore shown bold.

The behaviour of crystals oriented at or near a boundary between regions in fig. 3 is of interest and enables one to define three types of boundary which may be termed *stable*, *unstable* and *permeable*. These will be illustrated for the case of tensile tests with reference to fig. 3a. Owing to deformation by single slip in tension the specimen axis tends to rotate along a great circle of the stereogram towards the operative slip direction, and an indication of the relevant rotation is given by the arrows on the contour plot. In the case of an *unstable* boundary, denoted by "u" in the figure, the rotation on either side is away from the boundary so that a situation in which slip occurs on two systems is unlikely to arise. Two such boundaries meet at the [1 1 1] pole in fig. 3a and a third divides the regions marked A and C. For *stable* boundaries, marked "s", the rotations are towards the boundary from both sides so that when a specimen axis reaches such a boundary double slip should occur. The axis then, in principle, rotates along the boundary until it becomes coplanar with the two slip directions. Thus the two stable boundaries in fig. 3a have terminal poles at $[2\,\bar{1}\,\bar{1}]$ and $[1\,1\,\bar{2}]$, the corresponding rotations being indicated by arrows. Finally the rotations may be towards a boundary from one side and away from it on the other, giving rise to a *permeable* boundary, represented by "p". In this case a specimen axis will tend to traverse the boundary resulting in a change of slip system but, in principle, the double slip situation will only arise instantaneously as the axis crosses the boundary. An example of this type of boundary divides the regions marked A and B in fig. 3a.

The deformation geometry for crystalline mercury described above applies equally well to specimens deformed in uniaxial and bend tests. However, additional constraints are clearly imposed by four-point bending and these will now be discussed. In an analysis of plane plastic strain, to be described in detail elsewhere [13], it has been shown that three independent shears are in general necessary to accommodate pure bending strains in a single crystal. For mercury only two of the three $\{1\,1\,\bar{1}\}\langle 1\,\bar{1}\,0\rangle$ slip systems are

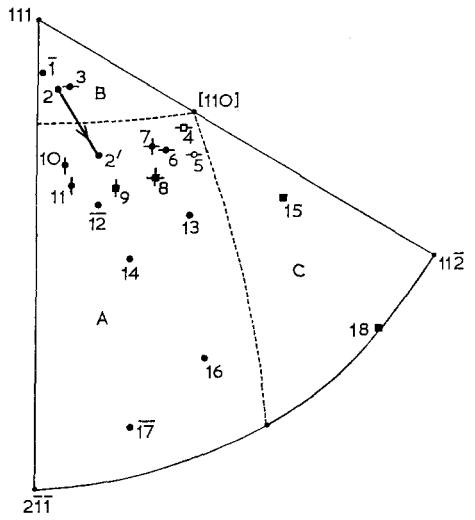

Figure 5 Orientations of the axes of the specimens subjected to uniaxial tests. Circular and square symbols represent crystals of circular and square cross-section respectively and specimens tested in compression are distinguished by bars above their numbers. Symbols with horizontal and vertical bars indicate crystals which twinned and kinked respectively, and open symbols crystals which did not apparently slip prior to twinning. The remaining specimens all deformed by slip on the most highly stressed variant of the $\{11\bar{1}\}\langle 1\bar{1}0\rangle$ system the regions for the three different variants with slip directions A, B and C being indicated.

independent so that in general additional deformation modes must operate in bent crystals. In particular twinning, kinking and wavy slip are all likely to occur in specimens which in uniaxial tests would deform entirely by crystallographic $\{11\bar{1}\}\langle 1\bar{1}0\rangle$ slip. However, for particular orientations, bending may be accommodated by either one or two shears. For the case of $\{11\bar{1}\}\langle 1\bar{1}0\rangle$ slip these orientations arise when the bend axis is parallel to $\langle 112\rangle$ and $\langle 1\bar{1}0\rangle$ respectively; they are shown schematically in figs. 4a and b. It is interesting that to a close approximation these same bend axes are also appropriate for single and double shear bending respectively when the operative deformation mode is '$\{\bar{1}\bar{3}5\}$' twinning. However as twinning is a unidirectional process these mechanisms would have to be restricted to either the tension or compression face. The choice between slip and twinning as the operative mode would then depend on the relative values of the Schmid-factors, which can be deduced from figs. 2 and 3. The case of $\langle 011\rangle$ type slip must also be considered although it is not normally favoured at 77° K. Indeed it may well occur in specimens with axes near [111] for which the Schmid-factors for $\langle 1\bar{1}0\rangle$ slip and '$\{\bar{1}\bar{3}5\}$' twinning are all small. The bend axis would then once more be $\langle 01\bar{1}\rangle$ with an effective wavy slip plane, appropriate for this direction, near $\{100\}$.

3. Experimental Techniques

Single crystals of mercury of square or circular cross-section were grown from singly distilled mercury containing < 3 ppm non-gaseous impurities. Both types of crystal were grown by a modified Bridgman technique to be described in detail elsewhere [14]. The flat surfaces of the square crystals were particularly useful in the characterisation of the morphology of the deformed crystals, whereas identification of the operative shear directions was simpler on the cylindrical samples. The diameter of these and the facial dimension of the square crystals were both 6 mm and the crystals were grown at least 7 cm long for tension and bending tests and 5 cm long for compression tests.

After examination under polarised light in order to detect grain boundaries, the crystals were oriented using the Laue X-ray back-reflection method, indexing of the patterns being performed using the table of crystallographic angles of mercury computed by Bacon *et al* [2]. The crystals were then annealed in a bath of ethyl alcohol and solid CO_2 at 200° K for between one and four weeks prior to testing. The crystals were then carefully dried and slowly cooled to 77° K before mounting in the appropriate precooled deformation jig. The whole assembly was then immersed in a bath of liquid nitrogen and the specimen deformed. Examination of the surfaces of the crystals on completion of the tests was carried out with an optical microscope fitted with a goniometer eyepiece to permit trace analysis measurements to be made. The specimens were held just above the level of the liquid refrigerant, which was either liquid nitrogen or cold ethyl alcohol. Trace analysis of these deformed crystals was then carried out in the manner described in previous papers [4, 9,] the estimated accuracy being 2° and 4° for planes and directions respectively.

In the case of the uniaxial tests, correct alignment between the crystals and the chuck pieces was achieved by laying the latter in an accurately machined V-block. The compression attachment was of conventional design although allowing no sideways movement during deformation. These tests were performed on a Tenso-

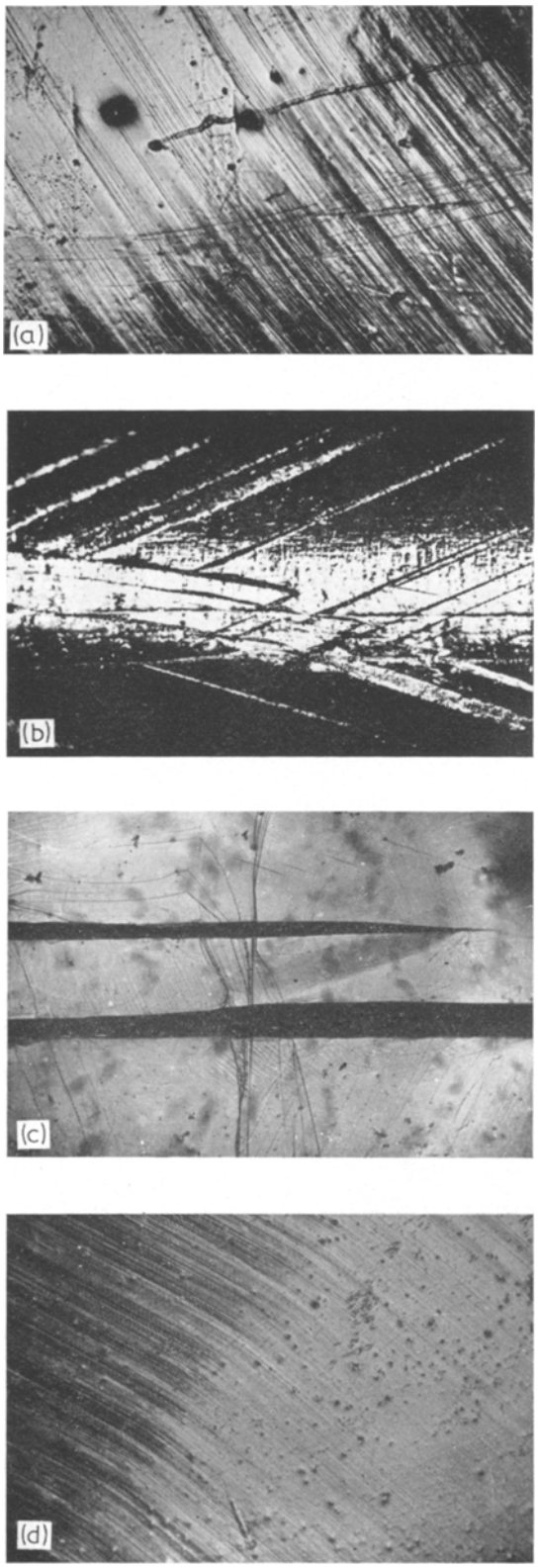

meter machine at a cross-head speed of 4 mm min^{-1} for all but two crystals, where 16 mm min^{-1} was used. The load-extension curves were recorded, the tests often being stopped in the immediate post-yield region to identify the operative deformation mode prior to recording the curves more fully. Departure from linearity of these curves was assumed to indicate the onset of plastic flow. Unfortunately, reliable load-extension curves for the crystals tested in compression were not readily obtained due to icing of the runners of the jig. The bending tests were carried out in a four-point bending jig, the spans of the inner and outer edges being 2 cm and 6 cm respectively. In these tests the top surfaces of the specimens were observed during deformation using a × 10 objective. The displacements of the supports was recorded so that the maximum strains could be deduced but no attempt was made to determine the corresponding stresses.

4. Results

4.1. Uniaxial Tests

The crystallographic orientations of the axes of the eighteen specimens subjected to uniaxial tests at 77°K are shown in the standard stereographic unit triangle of fig. 5. The cross-section of five of these crystals, those denoted by square symbols and numbered 4, 8, 9, 15 and 18, was square. The remainder had circular cross-sections. The three specimens represented by numbers with bars, $\bar{1}$, $\bar{12}$ and $\bar{17}$, were tested in compression; the other crystals were all deformed in tension. Typical micrographs illustrating the observed slip, twinning and kinking modes of deformation are given in fig. 6. The slip lines in general formed in bands approximately 600 μm across, the regions between the bands filling up at higher strains. However, the distribution was more homogeneous in crystals having higher values of the Schmid-factor. The general morphology of the twins was similar to that reported earlier [9, 10], for crystals deformed either by impact or bending. In particular, cross-twinning between complementary pairs of twins occurred on crystals in which two variants of the twinning

Figure 6 Micrographs illustrating (a) crystallographic (A) A or $\{11\bar{1}\}\langle 1\bar{1}0\rangle$ type slip (× 60), (b) profuse '$\{\bar{1}35\}$', twinning (× 30), (c) accommodation kinking between two twins (× 60) and (d) macroscopic A (A) or $\{1\bar{1}0\}'\langle 33\bar{2}\rangle'$ kinking (× 60) on crystals of circular ((a) and (b)), and square ((c) and (d)) cross section deformed in tension.

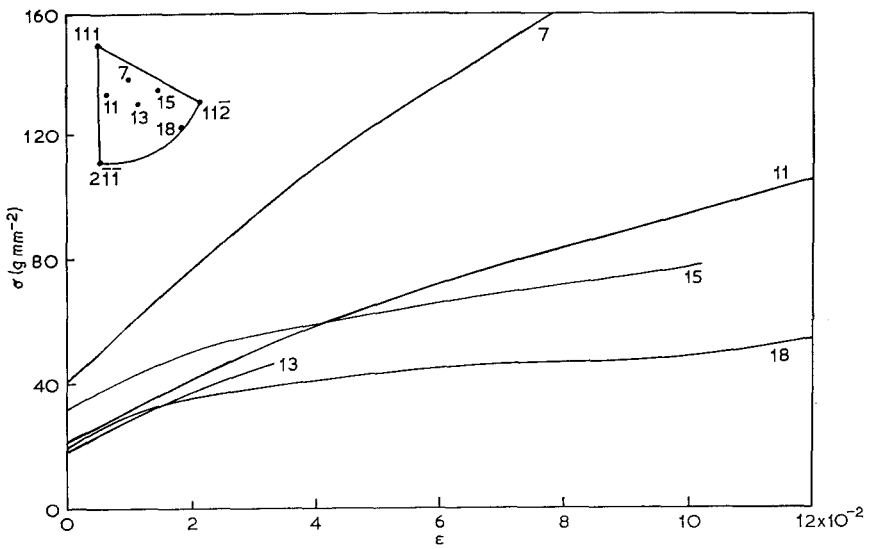

Figure 7 Resolved shear stress-strain curves for five crystals which deformed predominantly by slip in tension. The orientations of the axes of the five specimens are indicated on the inset.

mode operated. Accommodation kinking was found to be associated with the tips of many twins and especially twin intersections. Macroscopic kinks were distributed approximately evenly along the gauge lengths of the appropriate specimens varying in number from five to ten and representing lattice rotations of up to about 15 degrees.

The predominant mode of deformation both in tension and compression was $\{11\bar{1}\}\ \langle 1\bar{1}0\rangle$ crystallographic slip. Only two specimens, 4 and 5, which are represented by open symbols in fig. 5, did not apparently deform by means of this mechanism. The operative variant of the slip mode was in all cases that predicted by the maximum Schmid-factor as demonstrated in fig. 5 by the regions A, B and C reproduced from fig. 3a. Six crystals, numbered 3, 4, 5, 6, 7 and 8 and denoted by symbols with horizontal bars grouped near the [110] pole, deformed by twinning on variant a′ of the '$\{\bar{1}\bar{3}5\}$' mode. It is clear from fig. 3 that this variant has the highest Schmid-factor for twinning in tension. Of these six specimens, 4 and 5, the two which showed no signs of prior slip, also twinned on the complementary variant a, which is also the second most highly stressed system. No twinning was observed in the specimens tested in compression. Macroscopic kinking occurred in five specimens numbered 7, 8, 9, 10 and 11 and represented by symbols with vertical bars grouped just above the centre of the triangle. These were all deformed in tension, the operative variant A (A) corresponding to the associated slip system.

The extent to which the specimens deformed by means of the different deformation modes varied considerably and further information is in some cases revealing. Thus, for example, although crystal 8 twinned, only one twin was present. Again although specimens 6 and 7 have similar

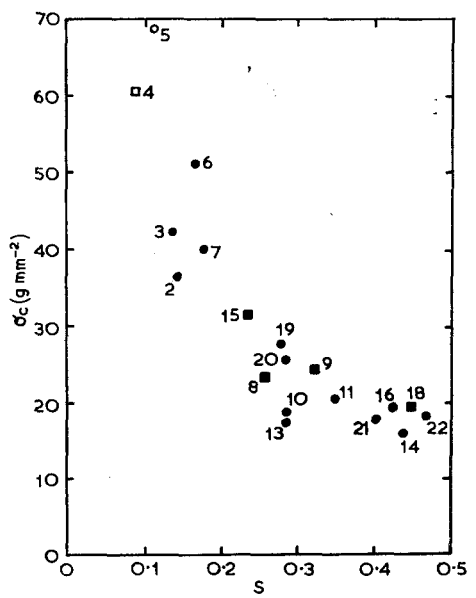

Figure 8 The critical resolved shear stress for slip, σ_c, as a function of Schmid-factor S for specimens tested in tension.

TABLE III Operative deformation modes, Schmid-factors and strains for the bent specimens

Crystal	*1*	*2*	*3*	*4*	*5*	*6*	*7*	*8*	*9*	*10*	*11*	*12*	*13*	*14*	*15*	*16*	*17*
S_A	02	*08*	*11*	*03*	**36**	**18**	*13*	*00*	*10*	*00*	*09*	12	**45**	**49**	47	43	**46**
S_B	05	**11**	**13**	05	35	*14*	02	12	08	*24*	24	*23*	14	*43*	45	*42*	**30**
S_C	03	02	00	02	12	05	*13*	**12**	**16**	24	*33*	**35**	*31*	06	*02*	*02*	16
S_a	07	04	01	**20**	$\overline{26}$	06	13	27	15	**26**	**18**	14	$\overline{30}$	$\overline{43}$	$\overline{47}$	$\overline{48}$	$\overline{43}$
S_a'	10	18	18	**24**	33	*35*	**37**	27	36	**28**	**35**	38	45	35	29	22	34
S_b	08	11	08	$\overline{04}$	28	00	$\overline{16}$	$\overline{25}$	$\overline{22}$	$\overline{37}$	$\overline{40}$	$\overline{40}$	$\overline{15}$	20	24	18	00
S_b'	00	$\overline{06}$	$\overline{06}$	$\overline{11}$	$\overline{29}$	$\overline{20}$	$\overline{17}$	05	$\overline{15}$	03	$\overline{02}$	$\overline{05}$	$\overline{38}$	$\overline{47}$	$\overline{49}$	$\overline{49}$	$\overline{48}$
S_c	00	$\overline{02}$	$\overline{01}$	$\overline{08}$	04	00	01	$\overline{05}$	03	04	15	18	37	19	**19**	**24**	35
S_c'	05	03	02	$\overline{05}$	01	$\overline{08}$	$\overline{20}$	$\overline{25}$	$\overline{25}$	$\overline{36}$	$\overline{40}$	$\overline{39}$	$\overline{15}$	09	**16**	**16**	06
S_β	**50**	*50*	*50*	—	—	—	—	—	—	—	—	—	—	—	—	—	—
ϵ	90	09	54	—	54	23	40	18	18	58	—	18	18	—	63	22	18

The Schmid-factors $S_{A,B,C}$ for crystallographic $\{1\,1\,\bar{1}\}\langle 1\,\bar{1}\,0\rangle$ slip, $S_{a,a',b,b',c,c'}$ for '$\{\bar{1}\,3\,5\}$' twinning and S_β for the three observed cases of [1 0 1] slip (relative to the maximum resolved shear stress plane) are given in units of 10^{-2}, negative values for the case of twinning being surmounted by bars. Predominant and secondary operative variants are shown by bold and italic numerals respectively. Maximum strains ϵ are in units of 10^{-3}.

orientations the former twinned after very little slip had occurred, but the latter only twinned after extensive slip and kinking. Specimens 2 and 3 also have similar orientations, but 3 twinned after prior slip while 2 hardened rapidly on testing. The lattice rotation associated with the deformation of this crystal by means of slip variant B resulted in the orientation of its axis rotating across the permeable boundary between regions B and A as indicated in fig. 5. However, not until the axis reached location 2′ was slip variant A detected. This was the only crystal tested which was observed to reach or cross a boundary between regions of the unit triangle in which different slip systems operate.

The stress-strain curves for specimens 7, 11, 13, 15 and 18, which are typical of the crystals which deformed predominantly by slip in tension, are given in fig. 7. Apart from specimen 7 and possibly 11, which kinked over most of the gauge length, they exhibit a low work-hardening rate. Crystal 7 also twinned at a higher stress than shown in the figure. The critical resolved shear stress for slip (c.r.s.s.) clearly varies considerably for these crystals. This is demonstrated more fully in fig. 8, where the c.r.s.s. for all thirteen crystals which deformed by slip in tension is given as a function of Schmid-factor. Also included are results for four cylindrical crystals, numbered 19, 20, 21 and 22, whose Schmid-factors were deduced from surface traces as their orientations were not uniquely determined by X-ray methods. In addition, minimum possible values of the c.r.s.s. for crystals 4 and 5 which did not apparently slip have been deduced from the stresses at which they were observed to twin. In general, the twinning stresses were so large compared with those for slip that no attempt has been made to represent twinned crystals in figs. 7 and 8. A summary of the data for the six relevant specimens is therefore given in table II. Stress-relaxations were observed when twinning occurred, being particularly large in the cases of crystals 4 and 5 where twinning was profuse. Audible clicks accompanied the twin bursts. When such a burst occurred the test was usually interrupted and the specimen surface examined. On re-testing crystals 4 and 5, twinning again occurred with no apparent slip and at a stress lower by about 20% than for the earlier burst. For the crystals that slipped before twin bursts were observed, further slip occurred on re-testing.

4.2. Bend Tests

The crystallographic orientations of the specimen and bend-axes of the seventeen crystals of square cross-section subjected to deformation by four-point bending at 77° K are shown in the standard stereographic unit triangles of fig. 9a and b. The predominant deformation mode in the regions of these specimens which experienced tensile stresses is indicated by different symbols in the figure. Note that six crystals, labelled *4*, *7*, *10*, *11*, *15* and *16* deformed primarily by '$\{\bar{1}\,3\,5\}$' twinning, one specimen, labelled *1*, by wavy $\langle 0\,1\,1\rangle$ slip and the remainder by crystallographic $\{1\,1\,\bar{1}\}\langle 1\,\bar{1}\,0\rangle$ slip. A complete list of the

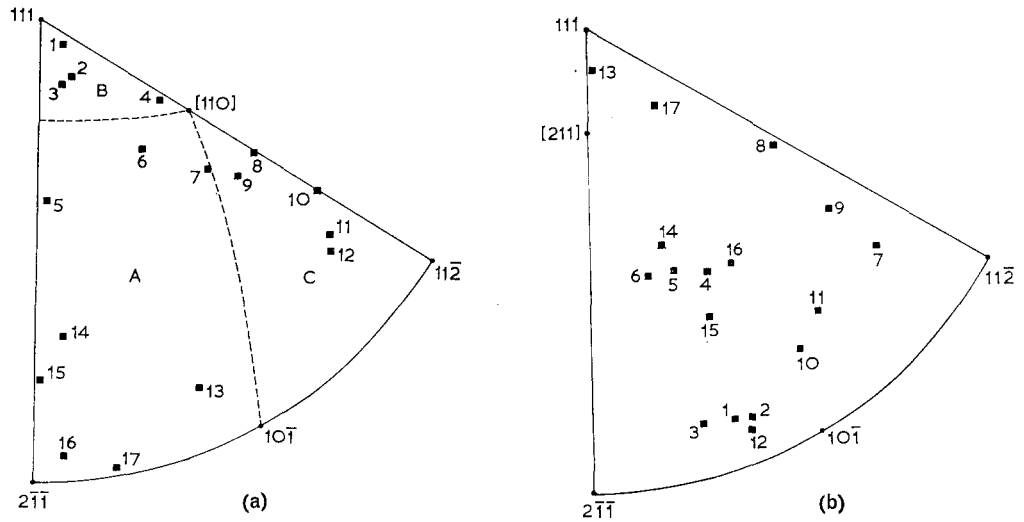

Figure 9 Orientations of (a) the specimen axes and (b) the bend axes of crystals deformed in four-point bending. The predominant deformation mode in the tensile region of the specimens represented by symbols with horizontal and oblique bars was a or '{$\bar{1}\bar{3}$5}' twinning and wavy α or ⟨011⟩ slip respectively. The remaining specimens deformed predominantly by (A) A or {11$\bar{1}$} ⟨1$\bar{1}$0⟩ slip, the operative variant having the maximum Schmid-factor as indicated in (a).

operative tensile deformation modes in these seventeen crystals is also given in table III, together with numerical values of the Schmid-factors for slip and twinning calculated on the basis of a pure tensile stress and, apart from three crystals for which the information is not available, the maximum strain. All deformation in the compressive regions was by slip. A composite micrograph, showing the tensile face and a side face of specimen *10* and clearly demonstrating the distribution of twinning and slip, is given in fig. 10.

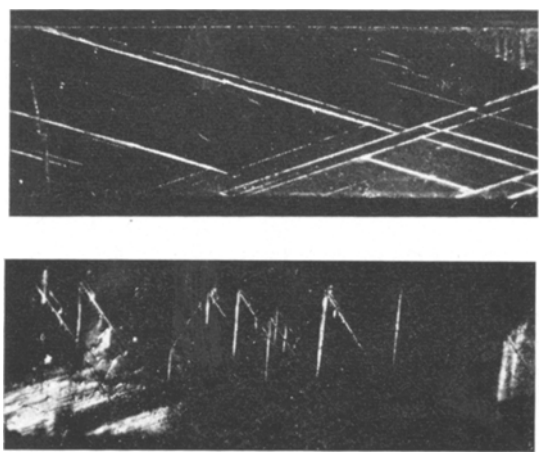

Figure 10 Micrographs of the tensile and side faces of specimen *10* following four-point bending. Note particularly the network of complementary twins which are restricted to the tensile region of the specimen. (× 3).

The most prominent deformation traces on the ten crystals which deformed primarily by {11$\bar{1}$} ⟨1$\bar{1}$0⟩ slip correspond to the variant with the largest Schmid-factor. None of these crystals was ideally oriented, with its bend axis parallel to ⟨112⟩, so that bending could occur by means of a single shear. However, as shown in fig. 9b, specimens *13* and *17* had approximately this orientation and the operative slip systems reflect this situation. Thus both specimens slipped primarily on the most highly stressed (A) A system which for an ideally oriented crystal would give pure bending. This was apparently the only operative system for specimen *17*, which probably therefore had a component of twisting in its macroscopic deformation. In specimen *13* this appears to have been avoided owing to the

TABLE II Data for the crystals which twinned in tension

Specimen	3	4	5	6	7	8
r.s.s.t. (a′)	66	200	204	152	328	66
S_a'	20	30	35	37	35	41
S_a	01	16	13	08	06	00
S	14	09	12	17	18	24

The resolved shear stress for twinning (r.s.s.t) is given in units of g mm^{-2} and the Schmid-factors for twinning on variants a ′and a and for slip on the most highly stressed variant of {11$\bar{1}$} ⟨1$\bar{1}$0⟩, represented by S_a', S_a and S respectively, are in units of 10^{-2}.

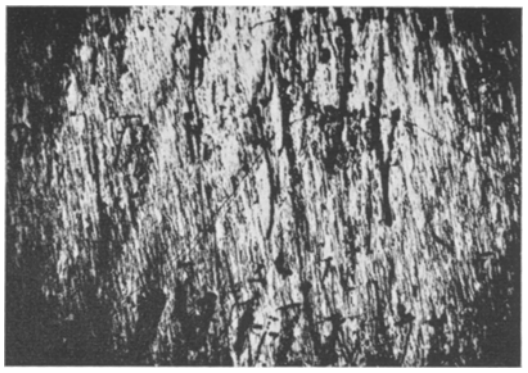

Figure 11 Micrograph of the tensile face of specimen *1* following four point bending. The wavy slip traces are due to $\langle 011 \rangle$ slip on the maximum resolved shear stress plane which is near $\{100\}$. (× 45).

occurrence of scondary (C) C slip which owing to the orientation of the specimen axis also had a high Schmid-factor. The best example of single-shear bending was however provided by crystal *1* which had its specimen- and bend-axes near $[111]$ and $[10\bar{1}]$ respectively. It was thus favourably oriented for plane plastic bending by means of shear on the (010) $[101]$ system. In practice this was accomplished by wavy slip in the $[101]$ direction, the average slip plane being approximately (010). The cross-slip process responsible for this result would clearly involve roughly equal amounts of slip on the $(11\bar{1})$ and $(\bar{1}11)$ planes. A micrograph of the tensile face of this specimen illustrating the nature of the wave slip traces is given in fig. 11. Similar wavy traces were also observed on specimens *2* and *3*, but in these cases the predominant deformation traces were variants of the $\{11\bar{1}\}\langle 1\bar{1}0\rangle$ slip system.

The only crystal oriented so that bending could be accommodated approximately by means of slip on two systems was specimen *12*, with its specimen- and bend-axes near $\langle 11\bar{2}\rangle$ and $\langle 1\bar{1}0\rangle$ respectively and indeed this is what occurred in practice. The remaining specimens all deformed by means of more complex mechanisms or did not conform to plane plastic bending, having for example a component of twisting in their deformation. The seven specimens which twinned were particularly interesting because, as indicated in fig. 10, the twins were restricted to the tensile regions of the bent crystals. Specimens *6* and *7* twinned on only one variant of the operative '$\{\bar{1}35\}$' mode, but, in the case of the former, twinning was a minor deformation mechanism. The operative mode was the one involving the highest Schmid-factor. The remaining five specimens each twinned on a complementary pair of twinning modes and apart from crystal *15* these were the first and second most highly stressed variants. In the case of crystal *15* the operative variants were in fact the third and fourth most highly stressed, but the only complementary pair involving two positive Schmid-factors. As indicated in table III accommodation slip on the corresponding $\{11\bar{1}\}\langle 1\bar{1}0\rangle$ slip system was associated with each pair of complementary twins despite the fact that the associated Schmid-factors were very small.

4.3. Discussion

The results presented in sections 4.1 and 4.2 have clearly demonstrated that the deformation modes of crystalline mercury exhibit a marked orientation-dependence. In addition, the operative modes were found in general to be consistent with those suggested by the geometrical analysis of section 2. The letter notation developed in the presentation of this analysis has greatly facilitated our interpretations. We have found that for both uniaxial and bending tests, when $\{11\bar{1}\}\langle 1\bar{1}0\rangle$ slip was the primary deformation system it was always the variant with the highest resolved shear stress which predominated. Thus the boundaries between regions A, B and C in figs. 5 and 9a are firmly established. Similarly, when twinning occurs, it is the mode with the largest Schmid-factor which tends to predominate, but the situation is here complicated by the phenomenon of complementary twinning, in which a pair of variants occurs together and by the unidirectional shear which leads to a marked asymmetry in the results of the bend tests. However, in the present paper we have concentrated our attention on the tensile regions of the bent specimens which can be compared most readily with the predominantly tensile deformation involved in the uniaxial tests. Nevertheless, a direct comparison between the uniaxial and bend test results of figs. 5 and 9a cannot unfortunately be made owing to the different distribution of specimen orientations in the two cases. Thus the specimen axes in fig. 5 tend to be concentrated in a region just above the centre of the unit triangle, whereas in fig. 9a it is the boundaries of this triangle which are favoured. This situation reflects the variable art of the crystal growing techniques adopted in this work, which is further illustrated by the orientation

distributions of Rider and Heckscher [4], and Crocker and Aytas [7]. It also emphasises the difficulty of investigating phenomena for a full range of crystallographic orientations for materials with low symmetry and hence with large unit stereographic triangles.

Although the operative $\{1\,1\,\bar{1}\}\ \langle 1\,\bar{1}\,0\rangle$ slip variant was correctly predicted by Schmid's law, nevertheless fig. 8 shows that a unique critical resolved shear stress (c.r.s.s.) for this type of slip, as measured in the tensile tests, apparently does not exist. Recently it has been claimed [15] that a satisfactory explanation of a similar phenomenon in single crystals of some body-centred cubic metals can be obtained by considering the normal stresses across the slip plane. However, for mercury the normal Schmid-factors increase as the specimen axis approaches $\langle 1\,1\,0\rangle$, the exact opposite to the behaviour required to account for the observations. A possible explanation of the remarkable results indicated in fig. 8 is that slip occurs at a critical strain rather than a critical stress and as mercury is elastically very anisotropic the stress corresponding to this strain will be a function of orientation. Unfortunately it is at present impossible to test this hypothesis unequivocally as the six elastic constants of mercury are not well established [16, 17]. In particular, the sign of one of the largest constants is uncertain. However, using simply the magnitude of this constant it has been shown [18] that the maximum and minimum possible shear moduli differ by a factor of 9 using compliance constants and 11 using stiffness, so that if a critical strain criterion is adopted then large variations of the observed resolved shear stresses at yield, as plotted in fig. 8, can be expected.

An alternative interpretation of these results may be reached when it is appreciated that it is the crystals near the permeable and stable boundaries of fig. 3a which have enhanced values of the c.r.s.s. These crystals are unlikely to deform by easy glide on yielding. In particular it is clear from figs. 3a and b that the Schmid-factor contours for variants (A) A and (B) B in the upper region of the unit triangle are almost coincident, so that the permeable boundary between regions A and B which geometrically is a line will in practice be a broad band in which double slip is very likely. Thus it may be that very rapid hardening occurs in these crystals so that the yield stresses deduced from the load-extension curves are much greater than the true yield stresses at which slip is initiated on the primary slip system. Indeed specimen 2, whose axis crossed the permeable boundary on testing, showed considerable latent hardening of slip variant A, illustrating the breadth of this boundary, and also work-hardened very rapidly. It follows from this argument that the true c.r.s.s. for $\{1\,1\,\bar{1}\}\ \langle 1\,\bar{1}\,0\rangle$ slip at 77°K is likely to be 18 ± 2 g mm^{-2}, the value consistently obtained for crystals with large Schmid-factors and hence with specimen axes remote from the possible double slip orientations. Rather disturbingly this value is considerably lower than the spread of results in the range 50 ± 17 g mm^{-2} reported by Rider and Heckscher [4] for crystals tested at 77°K and it is to be noted that several of their specimens had large Schmid-factors for $\{1\,1\,\bar{1}\}\ \langle 1\,\bar{1}\,0\rangle$ slip. The result of 16 ± 5 g mm^{-2} these authors obtained for crystals tested at about 200°K is also much larger than the value of 7 g mm^{-2} obtained by Greenland [19] at a similar temperature. These anomalies could be due to different impurity concentrations [19] and suggests that closer control over the purity of the specimens would be desirable in any future work on the measurement of flow stresses. It should be emphasised, however, that all of the crystals used in the present series of experiments were grown from the same stock of mercury and the behaviour illustrated in fig. 8 cannot be explained by variation of purity.

Considering now the twinning results, the most remarkable observation was the total absence of twins on the compression faces of the bent specimens. However, this strange result is very simply explained by comparing the Schmid factor contours of figs. 3a and e which are very similar. Thus if a c.r.s.s. for twinning exists, it need only be marginally greater than that for slip to exclude twinning from operating in compression. The situation is very different for twinning in tension. Thus as demonstrated by fig. 3c, for a large region of the stereographic unit triangle along the $1\,1\,1$-$1\,1\,\bar{2}$ boundary, the Schmid-factor for the most highly stressed a′ twinning variant is larger than that for the most highly favoured $\{1\,1\,\bar{1}\}\ \langle 1\,\bar{1}\,0\rangle$ slip system. Examination of the results presented in figs. 5 and 9a and of earlier results of Rider and Heckscher [4] indicate that this is indeed the region containing all but two of the specimen axes of crystals which twinned. About one-half of these crystals also twinned on the complementary twinning plane a, this being greatly assisted by the fact that this variant, as

indicated by fig. 3d, is the second most highly stressed. The accommodation effects at the line of intersection of a complementary pair of twins a and a′ also require slip on system A so that crystals with specimen axes lying in region A of fig. 3a in addition to region a of fig. 3d will be particularly well oriented for complementary twinning and the results are consistent with this view. The two twinned crystals whose axes do not lie near the 1 1 1-1 1 $\bar{2}$ boundary were *15* and *16* of the bend tests. This is largely due to the extra constraints associated with this type of testing as although in each case two slip systems with larger Schmid-factors were available, their operation could have resulted in considerable twisting of the specimens. It is particularly interesting that these crystals both twinned on the complementary pair of twinning variants c and c′ although in the case of specimen *15* two other variants a′ and b had larger Schmid-factors. However, the corresponding complementary variants a and b′ had negative factors which apparently prevented these twins from operating.

These results clearly show that any attempt to establish a criterion for the onset of twinning is beset with difficulties. Nevertheless, it is clear from the results of the tensile tests that for a given Schmid-factor, twinning is more difficult than slip. This is also clear from the shear stress results of table II. However, when slip precedes twinning, table II shows that no consistent value for the resolved shear stress of any subsequent twinning is obtained. Also, although similar values of about 200 g mm^{-2} are given for specimens 4 and 5 in table II, for which no prior slip was detected, the mechanism is likely to be influenced by the operative complementary twins. Again these crystals have orientations in the region for which enhanced resolved shear stresses for slip were obtained. It has been suggested above that these may result either from anisotropic elasticity, influencing a controlling critical strain criterion, or from very rapid hardening due to multiple slip obscuring the true yield point. These effects will also influence the nucleation of twins for which the operation of interacting slip systems is known to be important in other materials [20].

Slip in the $\langle 0\,1\,1 \rangle$ direction was not observed at 77°K by Rider and Heckscher [4] who therefore deduced from the relative Schmid-factor values that the ratio of the c.r.s.s. for $\{1\,1\,\bar{1}\}$ $\langle 0\,1\,1 \rangle$ and $\{1\,1\,\bar{1}\}\langle 1\,\bar{1}\,0 \rangle$ slip was at least 4 at this temperature. Crystal 1 of our uniaxial tests which was tested in compression and slipped on $\{1\,1\,\bar{1}\}\langle 1\,\bar{1}\,0 \rangle$ confirms this minimum value but one of the most surprising features of the present series of experiments was the observation of $\langle 0\,1\,1 \rangle$ slip in specimens *1*, *2* and *3* of the bend tests. Indeed, the predominant slip in specimen *1* was in this direction. This suggests that the ratio of the critical stresses is less than 8. However, as the slip plane of this crystal was non-crystallographic, as illustrated by fig. 11, this value is questionable, and, as shown by table III, would become 10 if the stress is resolved on the operative maximum resolved shear stress plane, which was near $\{1\,0\,0\}$. When interpreting results on specimens bent at about 200°K, Crocker and Aytas [7] have argued that it is the nucleation of $\langle 0\,1\,1 \rangle$ slip on a crystallographic $\{1\,1\,\bar{1}\}$ plane that appears to be critical and deduced a unique value of 1.3 for this ratio which again was consistent with the range of 1.2 to 2.0 given by Rider and Heckscher [4].

Apart from a brief mention of surface features which Rider and Heckscher [4] thought were kink bands, kinking in mercury has not been discussed previously. As stated in the introduction of the present paper the crystallography of these kinks is particularly interesting as the effective shear direction is irrational. This topic will therefore form the basis of a separate publication [12] and we shall here concentrate on the orientation dependence of the specimen axes of the crystals which kinked macroscopically in the uniaxial tests. These are all concentrated in the upper part of region A in fig. 5. Their Schmid-factors for slip on system A are all approximately 0.25 but this value would tend to increase slowly as the specimen axes rotate, in the direction of the bold arrow in fig. 3a, under the action of easy glide if this were distributed uniformly over the length of the specimen. However, if slip on system A is concentrated in a particular region of a crystal, as it may be following strains of a few per cent and the associated hardening, the effective Schmid-factor in this region will be increased by the subsequent rotation, causing further localised slip and the development of macroscopic kink bands. In practice this is what invariably occurs in these specimens so that kinking is a significant deformation mode of mercury crystals. Note particularly that the fact that these kinks occur in tension is in no way anomalous. Indeed, the contours of fig. 3a suggest that in compression, when the specimen axis rotates towards the slip

plane normal, kinking is unlikely in crystalline mercury.

It is interesting that the kink bands observed in the present work were very similar to features photographed by Greenland [21] and reported to be twins. Rider and Heckscher [4] have also noted that features they observed on some of their specimens tested at about 200°K and interpreted as kinks were similar in appearance to some of the twins reported by Andrade and Hutchings [22]. In fact no twins have been recorded during the recent series of investigations [4, 7] on crystals deformed near 210°K, the temperature used in the early work [21, 22]. It is indeed remarkable that so many of the conclusions of this work [21, 22], which has been so stimulating to our own research, are now known to be incorrect. This was largely due to the fact that the crystals were not oriented using X-rays and resulted in incorrect indices being given for the slip plane, the predominant slip direction and the twinning mode, and it now appears that at least some of the "twins" were in reality kinks. Nevertheless the many beautiful micrographs presented with these early papers contain a wealth of morphological information which we are only just beginning to fully appreciate.

5. General Discussion

In previous sections of this paper we have made little reference to crystalline materials other than solid mercury but in this final section we shall concentrate our attention on how our results and interpretations are related to the general understanding of the mechanical properties of materials. To do this perhaps one's first inclination is to compare results on crystalline mercury with those on the other metals of rhombohedral symmetry, bismuth, antimony and arsenic [23]. However, the axial angle of the unit cell of all these metals is less than 90° rather than greater than 90° as in the case of mercury. In addition, their crystal structures involve two atoms being located at each point of the Bravais space lattice rather than one. Thus it is not surprising that the deformation modes of mercury are completely different from those of the other rhombohedral metals and it becomes meaningless to attempt to compare the dependences of these modes on orientation. In any case, unfortunately, little information on orientation dependence appears to be available for these other metals. The mercury structure is sometimes referred to an hexagonal basis [9] so that comparison of our results with those on hexagonal close packed metals might seem an attractive approach. However, these metals again have double lattice structures and the stacking sequence of the close-packed basal planes is two-fold rather than three-fold as in the case of the corresponding $\{11\bar{1}\}$ planes of mercury. Hence, many of the operative shear planes in these metals are rational but corrugated, whereas in mercury the operative planes are either perfectly smooth or irrational. In addition the deformation of h.c.p. metals is usually dominated by the basal plane or by the close packed directions it contains, a situation which has no parallel in crystalline mercury. Deformation of h.c.p. metals on the basal plane may of course be constrained [24] but any investigation of orientation-dependence must then inevitably be strictly limited.

A more fruitful approach may thus be to compare the deformation of mercury with that of other metals with single lattice structures, such as face-centred and body-centred cubic. Indeed, the reason we originally chose a face-centred rhombohedral unit cell for mercury, rather than the basic primitive rhombohedral cell, was to facilitate comparison with the f.c.c. metals. Such a comparison at first seems worthwhile as the mercury shear planes and directions for slip, twinning and kinking all degenerate to the corresponding f.c.c. elements on relaxing the mercury axial angle of about 98° to 90°. However, there are anomalies such as the fact that the predominant $\langle 1\bar{1}0\rangle$ slip direction is not the closest-packed direction and the twinning mode does not have the smallest possible shear strain compatible with no atomic shuffling. Body-centred cubic crystals may also be referred to a primitive rhombohedral unit cell of axial angle 99.5°, and therefore their deformation modes compared directly with those of mercury for which the corresponding angle is 70.8°. The exercise does not produce a useful correlation owing to the large differences between the axial angles but, as noted by Greenland [21], the morphologies of the mercury deformation traces and those of some b.c.c. metals and alloys are remarkably similar. This applies particularly to non-crystallographic slip traces [7]. The operative mechanisms in the two cases must, however, be very different and no conclusive evidence for slip asymmetry, now well-established in b.c.c. metals, has been discovered in mercury, although the crystallographic conditions for this phenomenon are satisfied by $\langle 011\rangle$ slip. The major difference

between mercury and the cubic metals, however, is the lower crystallographic symmetry of mercury, resulting in fewer variants of the operative deformation modes and a unit stereographic triangle which is four times as large as that for cubic crystals. Thus, for example, the use of the terms "primary", "critical", "cross" and "secondary" to describe different variants of the f.c.c. slip system are quite inappropriate for mercury and we have simply labelled the first and second most highly stressed systems "primary" and "secondary". Perhaps, therefore, the material whose deformation behaviour parallels that of mercury most closely is α-uranium, which has an orthorhombic structure, its unit triangle occupying one-quarter of the stereogram. However, this structure again has two atoms at each Bravais lattice point and this greatly influences the operation of its deformation modes. Nevertheless, like mercury, it slips in two different directions, twins and kinks profusely and the orientation dependence of the modes could be compared in detail [25, 26]. The general significance of the results on α-uranium, however, is that they demonstrate phenomena which in principle could occur in all crystalline materials but which had previously remained undetected or unexplored. For example, the occurrence of several twinning modes with irrational shear elements led to new interest in the crystallography of deformation twinning [27] and consequently the development of new general theories of this phenomenon [28, 29]. Similarly, cross-twinning mechanisms which were first discovered in α-uranium [25] and studied in detail have since been reported in many other metals, including mercury [10]. Thus we believe that the most valuable way of assessing our own results on crystalline mercury is to consider the general significance of the new and perhaps surprising information that we have presented in this paper.

First we wish to emphasise our use of Schmid-factor contour-plots for the first and second most highly stressed shear systems. These plots have enabled us to interpret in detail the majority of our results and to highlight certain crystal orientations associated with particular phenomena and mechanisms. This approach is important when discussing the orientation-dependence of the deformation modes of all crystalline materials but particularly those of low symmetry where the plots take on a complex and often fascinating form. The boundaries between the different regions in these plots, corresponding to double-shear orientations, are especially interesting and the *permeable* type of boundary has not, we believe, been considered previously. In the present paper the boundaries have arisen from the three-fold axis and mirror plane symmetry elements associated with the mercury structure. A general approach to the form of boundaries of this kind, analysing all possible symmetry elements for all thirty-two crystal classes, would be an attractive problem. Interpretation of the resulting contour maps might, however, necessitate collaboration with geomorphologists!

Secondly, we would like to stress the value of deformation by bending in the work we have reported here and elsewhere [7, 10]. This type of deformation was chosen largely because of its technical simplicity, which is clearly important when testing crystals which melt if they come within about 60°C of room temperature. We were well aware, however, that interpretation of the resulting deformation traces would be difficult for randomly oriented crystals. In practice the bent crystals showed some dramatic effects of asymmetry, particularly an absence of twinning on the compression faces, and has stimulated the development of a general analysis of plane plastic strain [13]. This analysis, which treats bending as a special case, considers orientations of crystals of any symmetry which may deform in plane plastic strain by means of the operation of a limited number of shear modes. It has been shown that in general five independent shear systems must be available but that for any particular orientation only three need operate. The special cases when only one or two systems are available have been examined in detail for a few materials including mercury and the f.c.c. metals [13]. Thus we have been able to interpret the results from our bent specimens in detail and would encourage others to adopt this form of testing.

Thirdly, we wish to highlight two aspects of our experimental results. The first of these is the apparent variation with orientation of the critical resolved shear stress for slip. This very surprising observation is, we consider, well-established but clearly requires further investigation. However, the point we wish to emphasise here is that it could probably not have been observed in a crystal of higher symmetry and hence with more variants of the operative deformation modes and a smaller unit stereographic triangle. For example, f.c.c. and b.c.c. metals each have twelve

variants of their operative $\{111\}\langle 1\bar{1}0\rangle$ and $\{1\bar{1}0\}\langle 111\rangle$ slip systems and the minimum Schmid-factor for the primary variant is in each case greater than 0.27. In mercury there are just three variants of the predominant $\{11\bar{1}\}\langle 1\bar{1}0\rangle$ slip system and the unit triangle is four times as large; consequently the Schmid-factor for the primary variant is zero for two distinct orientations of the specimen axis (figs. 3a and b). Note that it is for Schmid-factors between 0 and 0.27 that we have observed enhanced values of the c.r.s.s. Our tentative explanations of this phenomenon in terms of either a critical strain criterion or multiple shear-hardening are potentially of general application and require further study. Similarly, the interesting orientation-dependence of deformation kinking in crystalline mercury which occurs in specimens with Schmid-factors near 0.25 could not have been discovered in cubic metals. Also, because of the prevalence of these kinks we were led to investigating their crystallography in detail. In particular, by considering the significance of the irrational macroscopic shear direction, we have developed a general analysis of the crystallography of deformation kinking in crystalline materials [12]. This enables the operation of deformation-kinking modes to be rationalised and has particular relevance to deformation studies in b.c.c. metals.

Thus we have found our work on crystalline mercury fascinating in its own right and stimulating in terms of its significance to the general understanding of the mechanical properties of all crystalline materials. We trust that others will find the approaches adopted, interpretations advanced and general analyses developed of interest in considering their own materials problems.

Acknowledgements

We are indebted to Dr J. G. Rider, Mr I. Aytas, Dr N. D. H. Ross and Dr U. F. Kocks for valuable discussions and to the University of Surrey for financial support.

References

1. A. G. CROCKER, *J. Sheffield Univ. Metall Soc.* **8** (1969) 17.
2. D. J. BACON, F. HECKSCHER, and A. G. CROCKER, *Acta Cryst.* **17** (1964) 760.
3. A. G. CROCKER, F. HECKSCHER, and M. BEVIS, *Phil. Mag.* **8** (1963) 1863.
4. J. G. RIDER and F. HECKSCHER, *ibid* **13** (1966) 687.
5. J. S. ABELL and A. G. CROCKER, *Scripta Met.* **2** (1968) 419.
6. *Idem*, "The Mechanism of Phase Transformations in Crystalline Solids" (Institute of Metals, London, 1969) p. 192.
7. A. G. CROCKER and I. AYTAS, Report of Second International Conference on the Strength of Metals and Alloys (American Society of Metals, Cleveland, in the press).
8. A. G. CROCKER, F. HECKSCHER, M. BEVIS, and D. M. M. GUYONCOURT, *Phil. Mag.* **13** (1966) 1191.
9. D. M. M. GUYONCOURT and A. G. CROCKER, *Acta Met.* (1968) 523.
10. *Idem, ibid* **18** (1970) 805.
11. J. S. ABELL, A. G. CROCKER, and W. H. KING, *Phil. Mag.* **21** (1970) 207.
12. A. G. CROCKER and J. S. ABELL, to be published.
13. D. M. M. GUYONCOURT and N. D. H. ROSS, to be published.
14. F. HECKSCHER, D. M. M. GUYONCOURT, J. S. ABELL, and I. AYTAS, to be published.
15. R. B. ROY, *Scripta Met.* **3** (1969) 721.
16. E. GRÜNEISEN and O. SCKELL, *Ann. Phys.* **19** (1934) 389.
17. D. DETJE, G. L. SALINGER, and W. C. FULLIN, *J. Appl. Phys.* **41** (1970) 3189.
18. G. A. A. M. SINGLETON and A. G. CROCKER, to be published.
19. K. M. GREENLAND, *Proc. Roy. Soc. A* **163** (1937) 34.
20. J. W. CHRISTIAN, "The Theory of Transformations in Metals and Alloys" (Pergamon Oxford, 1965).
21. K. M. GREENLAND, *Proc. Roy. Soc. A* **163** (1937) 28.
22. E. N. DA. C. ANDRADE and P. J. HUTCHINGS, *ibid*, **148** (1935) 120.
23. E. O. HALL, "Twinning and Diffusionless Transformations in Metals" (Butterworths, London, 1954).
24. R. L. BELL, and R. W. CAHN, *Proc. Roy. Soc. A* **239** (1957) 494.
25. R. W. CAHN, *Acta Met.* **1** (1953) 49.
26. L. T. LLOYD and H. H. CHISWICK, *Trans. AIME* **203** (1955) 1206.
27. A. G. CROCKER, *J. Nucl. Mat.* **16** (1965) 306.
28. B. A. BILBY and A. G. CROCKER, *Proc. Roy. Soc. A* **288** (1965) 240.
29. M. BEVIS and A. G. CROCKER, *ibid* **304** (1968) 123.

Received 18 January and accepted 29 February 1971.